Journal of Natural Fibers

ISSN: 1544-0478 (Print) 1544-046X (Online) Journal homepage: www.tandfonline.com/journals/wjnf20

Graphene Oxide/Cuo-Coated Traditional Hanji Cellulose Paper for Wearable Thermal Heaters

Thirumalaisamy Suryaprabha, Omkar Y. Pawar, Heebo Ha, Baoyang Lu, Chunghyeon Choi, Jun Young Cheong, Sooman Lim & Byungil Hwang

To cite this article: Thirumalaisamy Suryaprabha, Omkar Y. Pawar, Heebo Ha, Baoyang Lu, Chunghyeon Choi, Jun Young Cheong, Sooman Lim & Byungil Hwang (2025) Graphene Oxide/Cuo-Coated Traditional Hanji Cellulose Paper for Wearable Thermal Heaters, Journal of Natural Fibers, 22:1, 2524001, DOI: 10.1080/15440478.2025.2524001

To link to this article: https://doi.org/10.1080/15440478.2025.2524001

Published online: 04 Jul 2025.

JOURNAL OF NATURAL FIBERS
2025, VOL. 22, NO. 1, 2524001
https://doi.org/10.1080/15440478.2025.2524001

Taylor & Francis
Taylor & Francis Group

OPEN ACCESS Check for updates

Graphene Oxide/Cuo-Coated Traditional Hanji Cellulose Paper for Wearable Thermal Heaters

Thirumalaisamy Suryaprabha[a*], Omkar Y. Pawar[b*], Heebo Ha[a*], Baoyang Lu[c], Chunghyeon Choi[a], Jun Young Cheong[d], Sooman Lim[b], and Byungil Hwang[e]

[a]Department of Intelligent Semiconductor Engineering, Chung-Ang University, Seoul, Republic of Korea; [b]Graduate School of Flexible and Printable Electronics, LANL-JBNU Engineering Institute- Korea, Jeonbuk National University, Jeonju, Republic of Korea; [c]Jiangxi Province Key Laboratory of Flexible Electronics, Jiangxi Science & Technology Normal University, Nanchang, China; [d]James Watt School of Engineering, University of Glasgow, Glasgow, UK; [e]School of Integrative Engineering, Chung-Ang University, Seoul, Republic of Korea

ABSTRACT

The demand for lightweight, flexible, and energy-efficient thermal heaters is growing for applications in wearable technology, thermal management, and smart electronics. However, achieving stable and uniform heating performance under mechanical deformation remains a critical challenge for conventional flexible heaters. In this study, we developed an advanced Hanji-based thermal heater by integrating graphene oxide (GO) and copper oxide (CuO) coatings to enhance electrical conductivity and Joule heating efficiency. The synergistic interaction between GO and CuO facilitated superior charge transport and robust conductive networks, resulting in rapid and efficient electrothermal performance. The optimized GO/(10%)CuO-coated Hanji exhibited a low sheet resistance of 6.3 kΩ/sq and achieved a surface temperature of ~ 80 °C within 180 s under low voltage operation. Unlike conventional polymer-based flexible heaters, the Hanji-based heater maintained stable and uniform heating even under various bending conditions, demonstrating exceptional mechanical flexibility, durability, and reliability. Furthermore, its multifunctional capabilities were validated through effective deicing performance and wearable sensing applications, distinguishing it from commercial and state-of-the-art thermal heaters. These results establish GO/CuO-coated Hanji as a sustainable, high-performance material for next-generation flexible thermal management systems and multifunctional smart devices.

摘要

在可穿戴技术、热管理和智能电子领域，对轻便、灵活和节能的热加热器的需求正在增长. 然而，在机械变形下实现稳定和均匀的加热性能仍然是传统柔性加热器面临的关键挑战. 在这项研究中，我们通过整合氧化石墨烯（GO）和氧化铜（CuO）涂层来提高电导率和焦耳加热效率，开发了一种先进的韩基热加热器. GO和CuO之间的协同相互作用促进了卓越的电荷传输和稳健的导电网络，从而实现了快速高效的电热性能. 优化的GO/（10%）CuO涂层韩吉在低电压操作下表现出6.3 kΩ/sq的低薄层电阻，并在180秒内实现了~80°C的表面温度. 与传统的聚合物基柔性加热器不同，韩基加热器即使在各种弯曲条件下也能保持稳定均匀的加热，展现出卓越

KEYWORDS
Heaters; printing; graphene oxide; Hanji; flexible, wearable

关键词
加热器; 印刷; 氧化石墨烯; 韩集; 灵活; 可穿戴的

CONTACT Jun Young Cheong junyoung.cheong@glasgow.ac.uk James Watt School of Engineering, University of Glasgow, Glasgow G12 8QQ, UK; Sooman, Lim smlim@jbnu.ac.kr Department of Flexible and Printable Electronics, LANL-JBNU Engineering Institute, Korea, Jeonbuk National University, Jeonju 54896, Republic of Korea; Byungil Hwang bihwang@cau.ac.kr School of Integrative Engineering, chung-Ang University, Seoul 06974, Republic of Korea

*These authors contributed equally to this work.

Supplemental data for this article can be accessed online at https://doi.org/10.1080/15440478.2025.2524001

的机械灵活性、耐用性和可靠性. 此外，通过有效的除冰性能和可穿戴传感应用验证了其多功能能力，使其与商用和最先进的热加热器区别开来. 这些结果使GO/CuO涂层韩吉成为下一代柔性热管理系统和多功能智能设备的可持续、高性能材料.

Introduction

Portable and flexible electronic devices have garnered significant attention in recent years, driving advancements across a wide range of applications, including biosensors, soft actuators, energy storage electrodes, nanogenerators, transistors, and human-machine interfaces (Huang et al. 2023; Xie et al. 2018; Yu et al. 2021;Choi et al. 2024; Kim et al. 2023). Among these, flexible electrothermal heaters have emerged as a critical technology due to their versatile applications in deicing systems for aircraft and automobiles, personal thermal management, wearable medical therapies, smart textiles, and advanced thermal control in next-generation electronics. Their ability to deliver rapid, uniform, and controllable heating makes them indispensable for high-performance and adaptive thermal solutions. The evolution of flexible heater technologies has enabled possibilities far beyond the capabilities of conventional electrothermal materials (Hu, Zhou, and Fu 2021; C.-L. Kim et al. 2017; Ha et al. 2023). Traditional ferrochromium alloys, commonly used in resistive heating, suffer from high density, limited mechanical flexibility, and susceptibility to oxidation, making them unsuitable for flexible and wearable applications. Another widely used material in commercial electrothermal devices is indium tin oxide (ITO), valued for its transparency and high electrical conductivity (Lin et al. 2017). However, its brittleness, high fabrication cost, and instability under mechanical deformation severely limit its applicability in flexible systems (Liu et al. 2021; Vertuccio et al. 2019).

To overcome these limitations, extensive research efforts have been devoted to identifying suitable replacements for commercial electrothermal materials. Among the promising alternatives, metal nanostructures have demonstrated excellent potential due to their high electrical conductivity, superior thermal stability, and mechanical flexibility (D. Lee et al. 2020; Tembei et al. 2020). However, challenges persist. For instance, in metal nanowires, the junctions between nanowires are prone to oxidation and electrical failure at elevated temperatures, compromising long-term durability. Meanwhile, metal nanoparticle-based heaters require high-cost noble metals, increasing production expenses (Cheng et al. 2022; H. Jiang et al. 2017; Liu et al. 2020; Wang et al. 2020).

The operation of flexible electronic heaters is based on the Joule effect, where an electric current driven by an external voltage flows through a resistive material, causing energy to dissipate as heat owing to inelastic electron – phonon collisions (Fang et al. 2022; Huang et al. 2023). This process effectively converts electrical energy into thermal energy, enabling precise and controllable heating. However, efficient thermal management and adaptability to mechanical deformations such as bending and twisting are crucial for reliable operation in wearable and flexible electronics. To achieve high-performance wearable thermal heaters, careful material selection and mechanical designs of the substrate play a vital role (Shi et al. 2019). The incorporation of conductive fillers onto flexible and durable substrates enhances mechanical stability and heat dissipation efficiency, ensuring stable operation under dynamic conditions (T.-H. Han et al. 2017; Tiwari et al. 2017).

In recent years, extensive research efforts have been dedicated to the development of flexible electrothermal heaters, flexible heaters have been fabricated using rubber or polymer substrates. For example, Zeng et al. (2023) developed a flexible heater using sulfonated poly(styrene – ethylene/butylene – styrene) as a substrate. The flexible heater achieved a surface temperature of approximately 68 °C within 20 s. Similarly, Choi et al. (2015) used a styrene – butadiene – styrene (SBS) thermoplastic elastomer to fabricate a stretchable heater that achieved a temperature of approximately 40 °C. However, many rubber-based materials lack breathability, leading to discomfort and limiting their suitability for prolonged use. Consequently, the choice of substrate for flexible heaters is crucial. An ideal substrate material must be flexible, provide an efficient thermal response, and possess a porous network structure (Xiang et al. 2023). Porous substrates enhance air permeability, improve wearer comfort, and maintain the structural integrity required for flexible wearable health and comfort devices (Ullah et al. 2022).

In recent years, paper-based substrates have garnered attention owing to their flexibility, light weight, cost-effectiveness, and eco-friendliness, which enable their use in flexible heaters, transistors, sensors, and energy devices (Jeong et al. 2024; Khadka, Kim, Park, et al. 2023; Khadka, Kim, Pradhan, et al. 2023). However, conventional paper exhibits low mechanical strength and chemical stability, limiting its durability in electronic applications. Unlike regular printing and writing paper, traditional Korean Hanji made from mulberry fibers offers distinct advantages, such as high molecular weight and long fiber length, which impart exceptional strength and stability to Hanji (Lim et al. 2023). In addition, the natural air permeability and porous structure of Hanji – historically valued for the ventilation in the doors of Korean houses (Hanok) – make it particularly suitable for modern electronics (Y. J. Kim et al. 2020, 2023). These properties ensure breathability and flexibility, making Hanji an ideal substrate for strain sensors, flexible heaters, and electrodes in energy storage devices (Jeong et al. 2024; J. Kim et al. 2024; Y. J. Kim et al. 2020). In our previous studies, we explored the potential of mulberry paper-based electrodes for eco-friendly energy storage applications and flexible electronics, comparing their performance with commercial cellulose papers. Our reliability studies demonstrated that mulberry paper exhibited an ultimate tensile strength of 32–40 MPa, significantly higher than the 11–12 MPa observed in commercial cellulose paper (Y. Han et al. 2024; Seo and Hwang 2019). Optical and scanning electron microscopy images revealed that the fiber diameter of mulberry paper was approximately 3.5 µm, whereas conventional cellulose paper exhibited a smaller fiber diameter of ~2.3 µm. Furthermore, mulberry paper was found to contain 1.49 times more holocellulose and 0.69 times less lignin compared to commercial paper. The higher lignin content enhances structural durability, while the abundant – OH functional groups in holocellulose facilitate stronger inter-fiber bonding through hydrogen bonding, thereby increasing the mechanical strength of the paper (Yun et al. 2018). These exceptional properties encouraged us to choose Hanji cellulose paper as a substrate for wearable thermal heaters. Among the materials used in paper-based electronics, graphene is particularly noteworthy owing to its exceptional electrical conductivity and flexibility (Chen et al. 2022; X. Jiang et al. 2016; Shin et al. 2023), making it an optimal choice for enhancing the performance of Hanji-based electronics.

Despite their numerous advantages, Hanji-based graphene materials face challenges in Joule heating applications because of their relatively high electrical resistance, which limits the heating efficiency by restricting the current flow required for consistent heat generation (H. Kim, Tiwari, and Kim 2021). This limitation affects both the heating speed and maximum achievable temperature. To address these issues, graphene oxide (GO) has been integrated with metal oxides such as ZnO, MnO_2, TiO_2, In_2O_3, and NiO in various electronics (Griffin et al. 2024). Copper oxide (CuO) effectively enhances the electrical and thermal conductivities of GO by increasing its electron mobility and creating additional conductive pathways, making it suitable for high-performance Joule heating applications (Akram et al. 2024; Mathesh et al. 2013; Rostami et al. 2021). The combination of CuO and GO offers distinct advantages, including enhanced thermal stability and electron transport, which are critical for flexible thermal heaters. To the best of our knowledge, no previous study has investigated the Joule heating performance of GO and CuO in flexible thermal heaters. This study addresses this gap by fabricating flexible thermal heaters using GO/CuO-coated mulberry paper.

Experimental

Materials

CuO (Sigma Aldrich, 98% powder), GO solution (GrapheneAll), and 1-methyl-2-pyrrolidone (NMP; Samchun, 99.5%) were used in the experiments.

Paper ink preparation

The printing ink was critical in the printing procedure. An appropriate amount of GO was added to the mortar and ground to remove any lumps. Subsequently, NMP was added to adjust the ink viscosity, ensuring that it was suitable for screen printing. The composite ink was then applied to the mulberry paper. GO/CuO composite inks were prepared using the same method with varying CuO contents (0, 5, 10, or 15 wt%).

Fabrication of GO/CuO-coated mulberry paper

The GO/CuO composite ink was coated onto mulberry paper using a screen printing method. Screen printing was performed using a screen printer (AMX-1242T semi-auto screen printer, Bucheon, Korea) equipped with a mesh (threads per inch: 400; opening: 830 µm; and mesh thickness: 390 µm). The prepared GO/CuO composite ink was applied to the mesh, and a squeegee was used to press the ink through the mesh on the mulberry paper in the desired design (2 × 2 cm square) at a 45° angle. The mesh speed was maintained at 60 mm s^{-1} to ensure a well-defined coating of the composite. This process was repeated using GO/CuO composite inks with different CuO contents (0, 5, 10, or 15 wt%). After printing, the GO/CuO-coated mulberry papers were dried at 150 °C for 3 h. The dried papers were used in further investigations. The printing parameters are maintained throughout the process (Table 1).

Characterization

The surface morphologies and microstructures of both pristine and coated mulberry papers were examined using field-emission scanning electron microscopy (FE-SEM; Carl Zeiss, SIGMA 300, Oberkochen, Germany). The elemental composition and mapping of the coated mulberry paper were analyzed using energy-dispersive X-ray spectroscopy (EDX; Sirion, FEI). Fourier transform (FTIR) spectra of the samples were recorded in a scanning range of 4000–400 cm^{-1} (Nicolet 6700 infrared spectrometer). X-ray diffraction analysis of Hanji samples was performed using an X-ray diffractometer (XRD; New D8-Advance, Bruker-AXS, USA).

Surface resistance was measured at room temperature using a digital multimeter (15B +600 V CAT III; Fluke, USA). Measurements were performed at five different locations on each sample, and the average value was used to calculate the electrical conductivity. The strain-sensing performances of the coated mulberry papers were evaluated using a high-resistance meter (6517 B, Keithley, USA) at room temperature. Surface temperature and thermal images were captured using a USB-based thermal camera (FL-IR Pro, FL-IR, USA). The water contact angles (WCAs) were measured with a goniometer (Drop Shape Analyzer DSCA100) using 5 µL of deionized (DI) water to assess hydrophobicity. All surface characterization and measurements were conducted at room temperature (~27°C) and a humidity range of 60–62% relative humidity (RH).

Results and discussion

Figure 1 illustrates the printing process used in these experiments. The prepared ink was first applied to the printing mesh, which was a crucial step in the process. The squeegee was then moved across the

Table 1. Printing parameters.

Parameters	Value
Ink viscosity	<2000 cP
Mesh count	threads per inch: 400
Mesh Tension	5–10 N/cm
Squeegee speed	250 mm/s
Off contact distance	1–2 mm

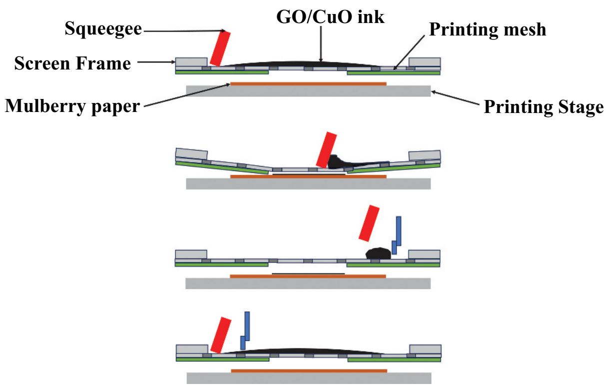

Figure 1. Schematic of the screen-printing process.

mesh following carefully defined parameters, such as speed, angle, and movement. As the squeegee traversed the mesh, it exerted pressure on the ink, forcing it through the mesh openings and onto the mulberry paper in a precise and controlled pattern – specifically a 2 × 2 square. After completing the forward motion, the squeegee returned to its starting position and the ink was redistributed. Once the external pressure was released, the ink was evenly spread over the mesh to ensure uniform coating in the next pass. This process was repeated systematically for printing mulberry paper using GO/CuO inks with various CuO contents (0, 5, 10, or 15 wt%) to ensure consistent results.

Surface characterization of Hanji samples

The chemical composition, crystal structure, and morphology of the flexible Hanji-based thermal heater are shown in Figure 2. FTIR spectroscopy was used to analyze the presence and interactions of functional groups in both pristine and coated Hanji samples. Figure 2a shows the FTIR spectra of Hanji, in which the characteristic bands of cellulose fibers are evident, with absorption bands observed in the range of 3400–3000 cm^{-1}, corresponding to the O – H groups inherent in the paper. Additionally, the absorption bands at 2919 and 2854 cm^{-1} can be attributed to the symmetrical stretching of C – H bonds in CH, CH_2, and CH_3 groups. Furthermore, the peaks corresponding to C – H bending vibrations at 1432, 1375, and 1319 cm^{-1}, as well as those corresponding to C – O – C stretching vibrations at 1163, 1034, and 894 cm^{-1}, are characteristic of Hanji, confirming its structural integrity and chemical composition (Jitjaicham and Kusuktham 2016; Y. J. Lee et al. 2024). The intensity of the absorption bands at 2919 and 2854 cm^{-1} of GO-coated Hanji slightly increased owing to the C – H stretching of methyl (CH_3) and methylene (CH_2) groups introduced by GO (Verma and Dutta 2015). This increase indicates the successful interaction between GO and Hanji paper, which enhances the functionality of the Hanji-based thermal heater. In contrast, upon the addition of CuO to GO, the intensities of the bands at 3373, 2919, 2854, 1432, 1163, and 1034 cm^{-1} (Mathesh et al. 2013; Menazea and Ahmed 2020; Xu et al. 2009) gradually decreased with increasing CuO content (5% and 10%). This decrease can be attributed to the partial masking of functional groups by CuO particles, while the absorptions at 606 cm^{-1}, 516 cm^{-1}, and 438 cm^{-1} indicate the stabilization of CuO through its interaction with the oxygen-containing functional groups of GO, such as hydroxyl and carboxyl groups (Kiran Kumar et al. 2017; Singh et al. 2016). GO contains oxygenated functional groups such as hydroxyl, epoxy and carboxyl group, interacts with CuO via electrostatic attraction, hydrogen bonding, and potential coordination between Cu^{2+} and oxygen groups. Simultaneously, the cellulose fibers in mulberry paper, composed of β(1→4) linked D-glucose unite with abundant hydroxyl group, from hydrogen bond with cellulose and GO and CuO. Under drying conditions, limited chemical bonding (e.g., esterification) may occur between cellulose and GO functional groups. Overall, the composite is held together by non-covalent interaction and forms

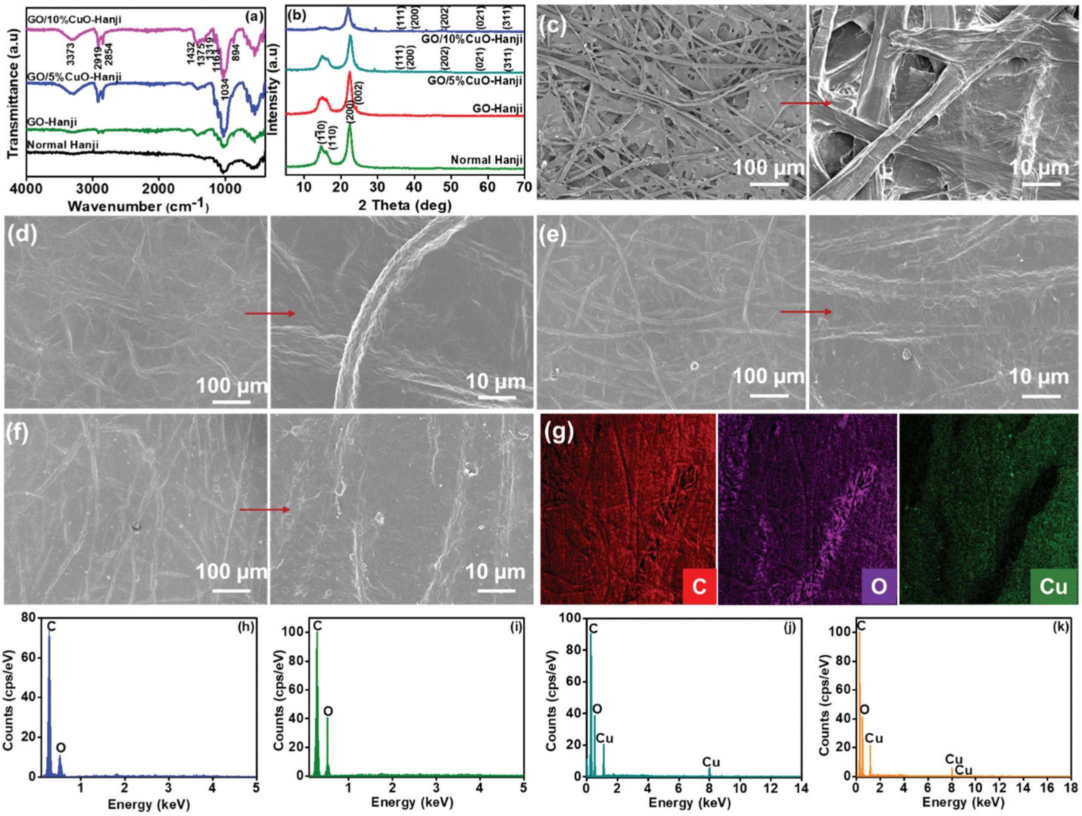

Figure 2. (a) Fourier transform infrared (FTIR) spectra; (b) X-ray diffraction (XRD) patterns of pristine and coated Hanji; scanning electron microscopy (SEM) images of (c) pristine Hanji, (d) GO-coated Hanji, (e) GO/(5%)CuO-coated Hanji, and (f) GO/(10%)CuO-coated Hanji; (g) energy-dispersive X-ray (EDX) spectroscopy mapping of GO/(10%)CuO-coated Hanji; and EDX spectra of (h) pristine Hanji, (i) GO-coated Hanji, (j) GO/(5%)CuO-coated Hanji, and (k) GO/(10%)CuO-coated Hanji.

a stable, layered structure with the flexibility of cellulose, the conductivity of GO and the semiconducting properties of CuO.

The XRD patterns of the Hanji-based thermal heaters and pristine Hanji are shown in Figure 2b. The XRD peaks at 14.6°, 16.2°, and 22.4° correspond to the (Γ10), (110), and (200) crystal planes of cellulose (Suryaprabha and Park 2023; Suryaprabha and Sethuraman 2017), respectively, confirming the crystalline structure of cellulose in Hanji. The XRD pattern of GO-coated Hanji exhibited a small diffraction peak at 24.9°, corresponding to the (002) (Krishnamoorthy et al. 2013) crystal plane, which is characteristic of the carbon structure of GO and the small diffraction peak observed at 10.1° corresponding to the (001) (Yasin et al. 2018) confirm the presence of GO on Hanji. This peak was consistently observed in all GO-coated Hanji samples, indicating the successful deposition of GO coating on the Hanji surface. The XRD patterns of GO/CuO-coated Hanji exhibited characteristic CuO peaks; however, the peaks were less intense owing to the low CuO content (5% CuO and 95% GO). The peaks at 35.2°, 39.1°, 48.6°, 58.6°, and 66.1° correspond to the (111), (200), (202), (021), and (311) crystal planes of CuO (Ganesan et al. 2020; Zhou et al. 2024), respectively. The intensity of these peaks slightly increased when the CuO content was 10%, confirming the successful integration of CuO with GO.

To evaluate the uniformity and continuity of the GO and CuO coatings on Hanji, the SEM micrographs of pristine and coated Hanji were acquired, as shown in Figure 2c–f. The SEM image of pristine Hanji (Figure 2c) revealed a crisscross fibrous structure. In contrast, the GO (100%)-coated Hanji exhibited a uniform wrapping of GO around the fibers, forming a continuous layer. The high-magnification images further confirmed the complete and homogeneous coverage of the GO layers on the fiber surfaces, demonstrating the effectiveness of the coating process (Figure 2d). The GO/(5%) CuO-coated Hanji surface appeared slightly rough with the presence of small CuO particles on its surface. The cross-sectional SEM image (Fig. S1) revealed a conformal coating of the GO/CuO composite along the fiber surfaces, indicating good adhesion and uniform distribution of the coating material on the Hanji surface. However, because of the low CuO content, the CuO particles were more distinctly visible in the high-magnification images and were sporadically distributed across the surface (Figure 2e). When the CuO content was increased to 10%, a denser distribution of CuO particles was observed with more prominent clusters on the fiber surfaces (Figure 2f). The high CuO content increased the surface roughness and contributed to the formation of additional conductive pathways, enhancing the thermal and electrical performances of the Hanji-based composite material. These observations confirmed the successful integration of CuO into GO and its potential to improve the functional properties of coated Hanji.

EDX mapping and elemental analysis were conducted to evaluate the distribution of GO and CuO on the Hanji surface (Figure 2g–k). The EDX mapping of GO/(10%)CuO-coated Hanji confirmed the uniform distribution of GO and CuO on the Hanji surface (Figure 2g). The EDX analysis of pristine Hanji revealed the presence of C and O, consistent with the cellulose structure of paper (Figure 2h). The increase in the C and O contents confirmed the successful coating of GO on Hanji fibers (Figure 2i). In the case of GO/(5%)CuO-coated Hanji, the Cu content was 4.2% (Figure 2j). When the CuO content was increased to 10%, the Cu content increased to 5.4%, indicating the enhanced incorporation of CuO into the GO matrix (Figure 2k) and confirming the effectiveness of the coating process. Following the surface morphology and elemental composition analysis by SEM & EDX, the thickness of the GO and CuO-modified GO coatings on Hanji paper was examined, as presented in Table 2.

Wettability Joule heating performances and reproducibility of Hanji samples

The combined SEM and EDX analyses revealed distinct morphologies and chemical compositions that influenced the wetting behavior of the Hanji samples. Figure 3a shows the WCA measurements of the samples. Pristine Hanji, characterized by the presence of abundant hydroxyl groups in the cellulose, exhibited a highly hydrophilic nature with a WCA of 0°, indicating complete wettability. The WCA of GO-coated Hanji increased to 74.6°, which can be attributed to the partial reduction of hydrophilic hydroxyl groups and the introduction of hydrophobic sp^2 carbon domains. The WCA of GO/(5%) CuO-coated Hanji further increased to 95.4°, indicating enhanced hydrophobicity owing to the presence of CuO nanoparticles, which disrupted the uniform surface energy of the composite. The WCA of GO/(10%)CuO-coated Hanji increased to 117.1°, indicating a transition toward highly hydrophobic behavior. This significant increase in hydrophobicity can be attributed to the combined effects of the surface roughness introduced by CuO particles and their inherently low surface energy, which reduced the affinity of the composite surface for water. In general, the deposition of metal and metal oxide nanoparticles onto various substrates significantly increases surface roughness by inducing micro- and nanoscale structural modifications. Previous studies have also demonstrated that CuO deposition enhances surface roughness while simultaneously lowering the surface energy of the underlying substrate (Aier and Dhar Purkayastha 2025; Dou et al. 2018; Ha et al. 2025; Ha et al.

Table 2. Thickness comparison of fabricated film.

Film	Thickness	Standard deviation
GO-Hanji	0.029	0.000816
GO/(5%) CuO	0.028	0.000831
GO/(10%) CuO	0.029	0.000416

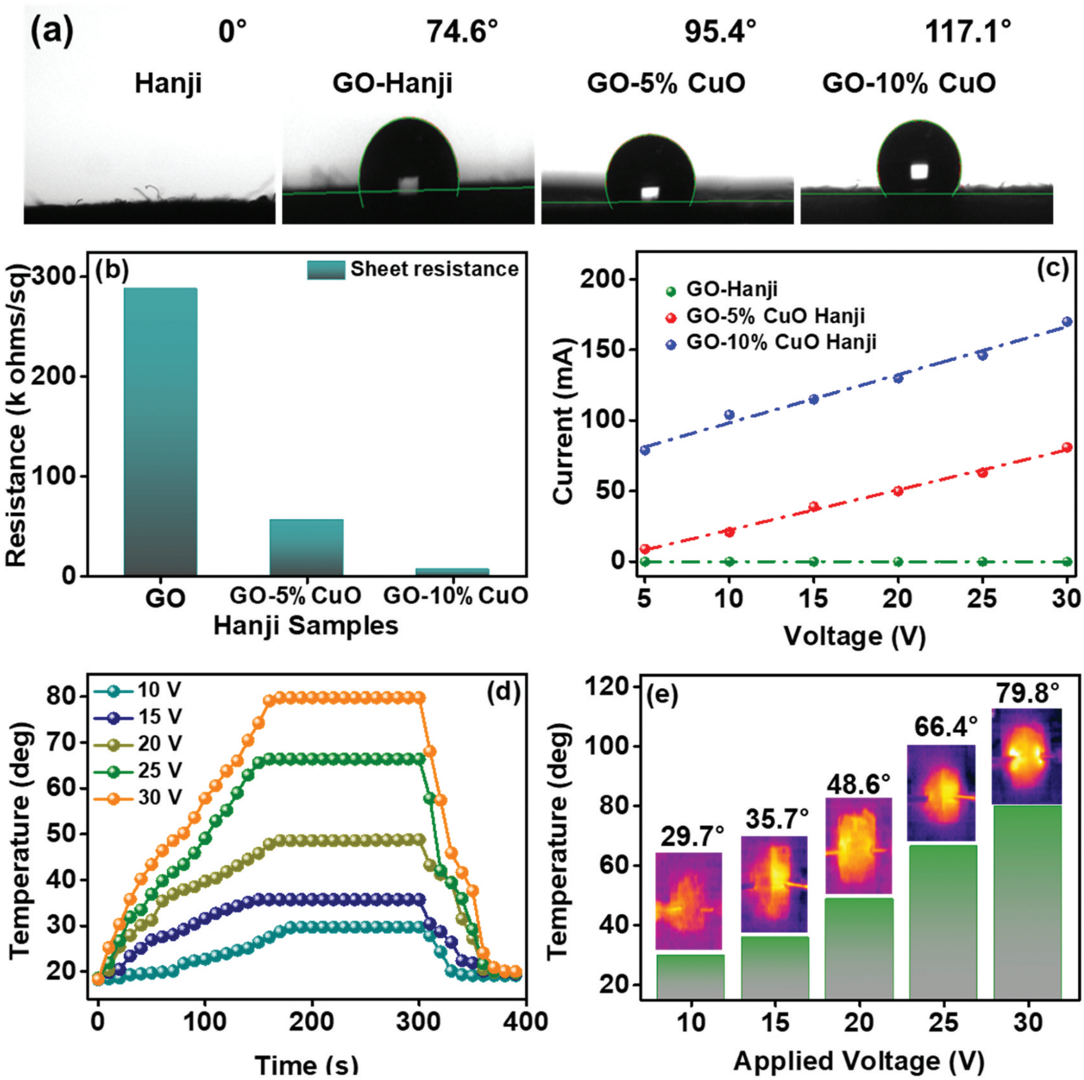

Figure 3. (a) Water contact angle (WCA) analysis; (b) Electrical conductivity measurements; (c) Current–voltage (I–V) curves of coated Hanji; (d) joule-heating performance of GO/(5%)CuO-coated Hanji; (e) relative surface temperature profile of GO/(10%)CuO-coated Hanji as a function of applied voltage and the corresponding thermal images.

2024). In this context, the incorporation of CuO particles onto the Hanji surface leads to the formation of a hierarchical micro-nanostructured topology, increasing surface asperities that trap air pockets and minimize direct water contact, consistent with the Wenzel and Cassie-Baxter wetting models. Furthermore, CuO inherently exhibits low surface energy, further reducing the wettability of the coated surface by limiting molecular interactions with water (Rajak et al. 2024). Collectively, these effects contribute to the observed improvement in the hydrophobicity of GO/CuO-coated Hanji. We have tested the layer integrity of GO/CuO coating on the Hanji paper by tape peeling test and virtual inspection showing no delamination after mechanical handling. The functional groups in GO likely enhanced interfacial bonding with CuO, contributing to this adhesion. The fabrication process was also repeatable, with coating from multiple batches due to same printing parameters. The thickness and electronic properties. Vernier caliper analysis showed minimal variation, with standard deviation in thickness within 5%, indicating reliable and reproducible fabrication process.

Figure 3b illustrates the sheet-resistance performance of the flexible Hanji-based thermal heater. To evaluate the electrical conductivities of the pristine and coated Hanji samples, we measured their surface resistances using a digital multimeter. Pristine Hanji is primarily composed of cellulose and is inherently insulating because of the absence of conductive pathways within its fibrous structure. The GO-coated Hanji exhibited a high electrical resistance of 288 kΩ/sq, which can be primarily attributed to the presence of numerous oxygenated functional groups in GO, which disrupted its conductive sp^2 carbon network and hindered electron mobility. The electrical resistance of GO/(5%)CuO-coated Hanji decreased to 55.8 kΩ/sq, which can be attributed to the formation of additional GO – CuO interfaces, where imperfect contact or scattering effects may initially hinder electron flow (Mathesh, et al. 2013). However, the electrical resistance of the GO/(10%)CuO-coated Hanji decreased significantly to 6.3 kΩ/sq. This reduction can be attributed to the improved dispersion of CuO particles, which created additional conductive pathways and enhanced the overall electron mobility within the composite. Increasing the CuO content to 15% resulted in a sheet resistance of approximately 5.8 kΩ/sq, which is approximately equal to that of the sample containing 10% CuO. This stabilization effect can be attributed to the saturation of the conductive pathways, where additional CuO does not substantially reduce the resistance, possibly because of particle agglomeration or limited interactions with the GO matrix. These results highlight the potential of optimizing the CuO content in GO/CuO coatings to improve the electrical performance of Hanji-based flexible thermal heaters.

The current – voltage (I – V) characteristics of the GO- and GO/CuO-coated Hanji samples are shown in Figure 3c. The linearity of the observed I – V curves indicates the Ohmic behavior of the coated Hanji samples, reflecting uniform electrical resistance across the material. This linearity confirmed the efficient charge transport through the coatings and validated the successful incorporation and continuity of the conductive layers on the Hanji surface. Achieving such uniform and stable electrical resistance is crucial for Joule heating because it ensures consistent heat generation across the entire surface.

High electrical conductivity and flexibility are essential properties of effective flexible thermal heaters (Chien et al. 2014). When external power is supplied, accelerated electrons collide with the atomic lattice (phonons) of the material, converting electrical energy into thermal energy via the Joule heating effect (Faruk et al. 2021). The Joule heating performance of GO/(10%)CuO-coated Hanji with dimensions of 3×3 cm^2 was evaluated by connecting it to a DC bias supply ranging from 10 to 30 V. The surface temperature distribution and voltage-dependent response of the samples were monitored with an infrared (IR) camera, providing insights into the thermal efficiency and stability of the materials under different operational conditions.

When external power was supplied, the surface temperature of the GO/(10%)CuO-coated Hanji began to increase after approximately 30 s and eventually reached maximum temperatures of approximately 29, 35, 48, 66, and 80 °C at applied voltages of 10, 15, 20, 25, and 30 V, respectively, within 180 s. An additional 30 s was required to reach a steady-state temperature. When the power supply was disconnected after 300 s, the surface temperature rapidly decreased and reached room temperature within 90 s (Figure 3d).

Figure 3e illustrates the linear and accelerated temperature increase for the GO/(10%)CuO-coated Hanji sample, with the corresponding thermal images revealing a gradual transition from red to yellow owing to the Joule heating effect. This electrochromic response highlights the efficient heat generation and uniform heat distribution facilitated by the CuO and GO coatings on Hanji.

The Joule heating performance of the GO/(10%)CuO-coated Hanji was further evaluated by applying a constant voltage of 30 V for 30 min to assess its thermal stability and long-term operational reliability. As shown in Figure 4a, the surface temperature of the GO/(10%)CuO-coated Hanji was stable without any noticeable decrease. The consistent performance demonstrated the excellent thermal stability and durability of the GO/CuO coatings under prolonged operation. These results highlight the robustness of the GO/CuO coatings, making them suitable for use in long-term thermal management and wearable heating devices.

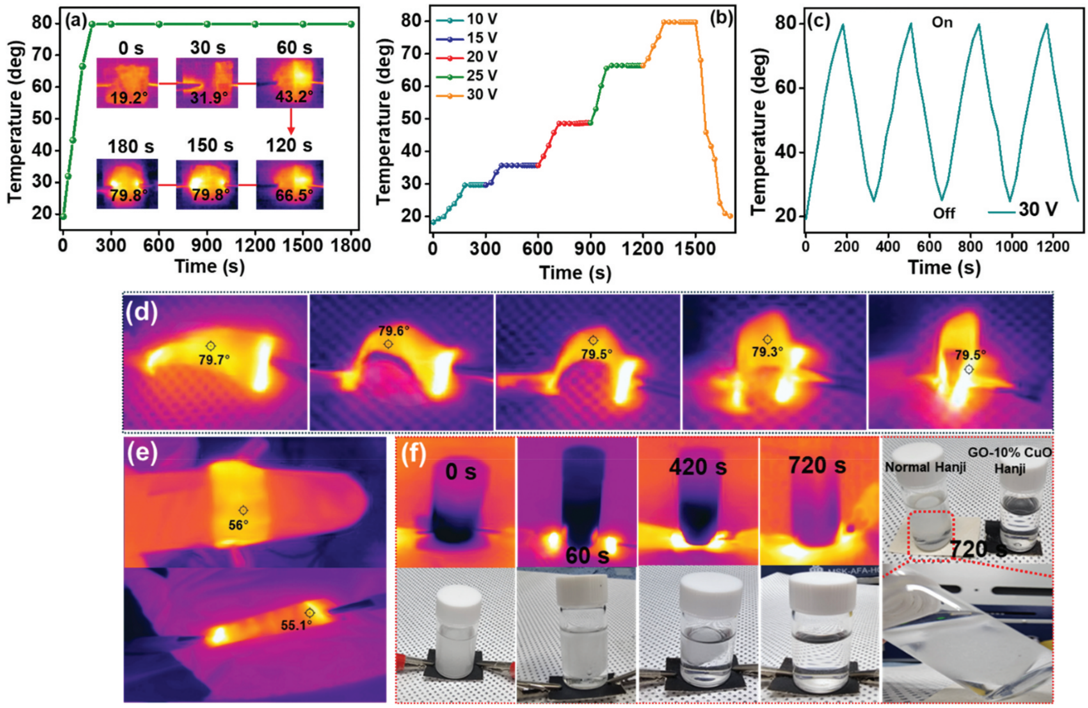

Figure 4. (a) Time-dependent surface temperature stability of GO/(10%)CuO-coated Hanji at 30 V in 30 min; (b) Controlled surface temperatures of GO/(10%)CuO-coated Hanji under gradient voltage; (c) stable cyclic performance of the Joule heating behavior of GO/(10%)CuO-coated Hanji; (d) thermal images of GO/(10%)CuO-coated Hanji affixed to a volunteer's hand; (e) de-icing performance of GO/(10%)CuO-coated Hanji; and (f) IR and digital photgraphic images of ice-melting performance of GO/(10%)CuO-coated Hanji at 30V.

The rapidity and controllability of the Hanji-based heater were further evaluated by applying voltages ranging from 10 to 30 V (Figure 4b). The results revealed that the Hanji-based heater exhibited consistent thermal responses at different voltages, achieving stable and efficient heating performance. This stability highlights the controllability of its electrothermal conversion capabilities. Additionally, upon disconnecting the power supply, the heater cooled efficiently, highlighting its excellent thermal responsiveness and making it suitable for advanced thermal management applications. The cyclic stability of the Joule heating performance of the Hanji-based heater was evaluated under an applied voltage of 30 V. The results demonstrated that the GO/(10%)CuO-coated Hanji exhibited excellent cyclic durability, maintaining stable and rapid heating performance over multiple heating cycles (Figure 4c). In addition, the electrical resistance was monitored over multiple repeated heating cycles and remained consistent with no significant changes, further confirming the electrical and thermal stability of the coatings on Hanji (Figure S2).

As mentioned earlier, the flexibility of Hanji is a crucial factor for its application in wearable heaters. To evaluate the effect of bending on the Joule heating performance, we examined the electrothermal responses of the GO/(10%)CuO-coated Hanji at various bending positions. Figure 4d shows the temperature changes at different bending positions. The IR images revealed no significant decrease or variation in performance, highlighting the robustness and consistent heat-generation capabilities of the wearable heater even under mechanical deformation.

To evaluate the suitability of the Hanji-based flexible heater for wearable applications, we attached the device to the index finger and the back of the hand of a volunteer to provide localized warmth while maintaining a comfortable interface. Upon applying the voltage, the surface temperature reached approximately 55–56 °C, effectively delivering heat to the wearer (Figure 4e).

Figure 4f shows IR images illustrating the deicing performance of the Hanji-based thermal heater. In this study, a 3 × 1 cm Hanji-based heater was connected to a DC power supply. A bottle containing approximately 10 mL of ice was placed on a coated Hanji-based heater and a pristine Hanji sample. When a voltage of 30 V was applied, the surface temperature of the coated Hanji-based heater increased to 78 °C within 5 min. Consequently, the ice on the thermal heater began to melt almost immediately and was completely melted within 12 min. In contrast, ice placed on a pristine Hanji sample took approximately 27–30 min to melt completely. These results highlight the superior efficiency and rapid thermal response of the coated Hanji-based thermal heater, demonstrating its potential for deicing applications. While the present work demonstrates the Joule heating capability of the coated layer, we acknowledge that coating thickness can significantly influence heating efficiency, response rate, and uniformity. A systematic study comparing different thicknesses will be necessary to optimize device performance and will be addressed in future investigations.

Wearable strain sensing performance of Hanji-based thermal heater

To explore additional applications of the Hanji-based heater, we evaluated the potential of the GO/(10%)CuO-coated Hanji as a wearable strain sensor, focusing on its ability to monitor human motion and physiological activities (Figure 5). For this evaluation, the Hanji-based sensor was affixed to the index finger and wrist of a volunteer's hand to test its sensitivity to small movements. During finger and wrist bending, the resistance of the Hanji sensor increased and returned to its original value once the movement ceased, demonstrating its excellent responsiveness to deformation. Notably, even during repeated bending and straightening, the GO/CuO-coated Hanji exhibited negligible changes in electrical resistance, indicating its high durability and stability under dynamic conditions (Figure 5a and b).

To further evaluate its ability to monitor larger movements, the Hanji sensor was attached to the neck and knee (Figures 5c and d). The recorded signal responses remained consistent, similar to those observed during the smaller movements, confirming the reliability of the sensor in detecting several motions. For each motion monitoring measurement, the Hanji sensor exhibited the response and recovery time of ~ 0.33 s- 0.39 s (Figure 5e-h). Furthermore, the GO/(10%)CuO-coated Hanji sensor demonstrated a gauge factor of 0.97, exhibiting low hysteresis and stable performance under varying strain conditions (Figure 5i and j). The strain sensing mechanism of the GO/CuO-coated Hanji sensor is governed by the dynamic modulation of its conductive network under mechanical deformation. Initially, the GO and CuO nanoparticles establish a well-percolated conductive network across the Hanji fibers, facilitating efficient charge transport. When subjected to tensile strain, the interconnected pathways undergo structural rearrangement, increasing interparticle distances and reducing the number of available conduction routes. This disruption arises from the mechanical mismatch between the rigid conductive nanomaterials and the flexible Hanji substrate, leading to slippage and partial debonding of GO and CuO particles. Consequently, the overall electrical resistance increases (Souri et al. 2020). Additionally, CuO, as a p-type semiconductor, plays a crucial role in modulating charge transport by altering carrier dynamics within the composite. The resistance change is further influenced by the tunneling effect, where increasing separation between adjacent nanomaterials introduces higher potential barriers for electron transport. Upon strain release, partial restoration of the conductive network occurs, facilitating a decrease in resistance and enabling the sensor to recover its original electrical properties (Khuje et al. 2024). These results highlight that the GO/(10%)CuO coating not only enhances the thermal properties of Hanji but also allows it to function as a wearable strain sensor for the real-time monitoring of human motion. It should be noted that GO can undergo partial reduction to reduced graphene oxide (rGO) during Joule heating under applied voltage, which may alter the electrical resistance. Although this effect was not quantitatively analyzed in the present study, it could influence the long-term resistance stability. Nevertheless, the coated

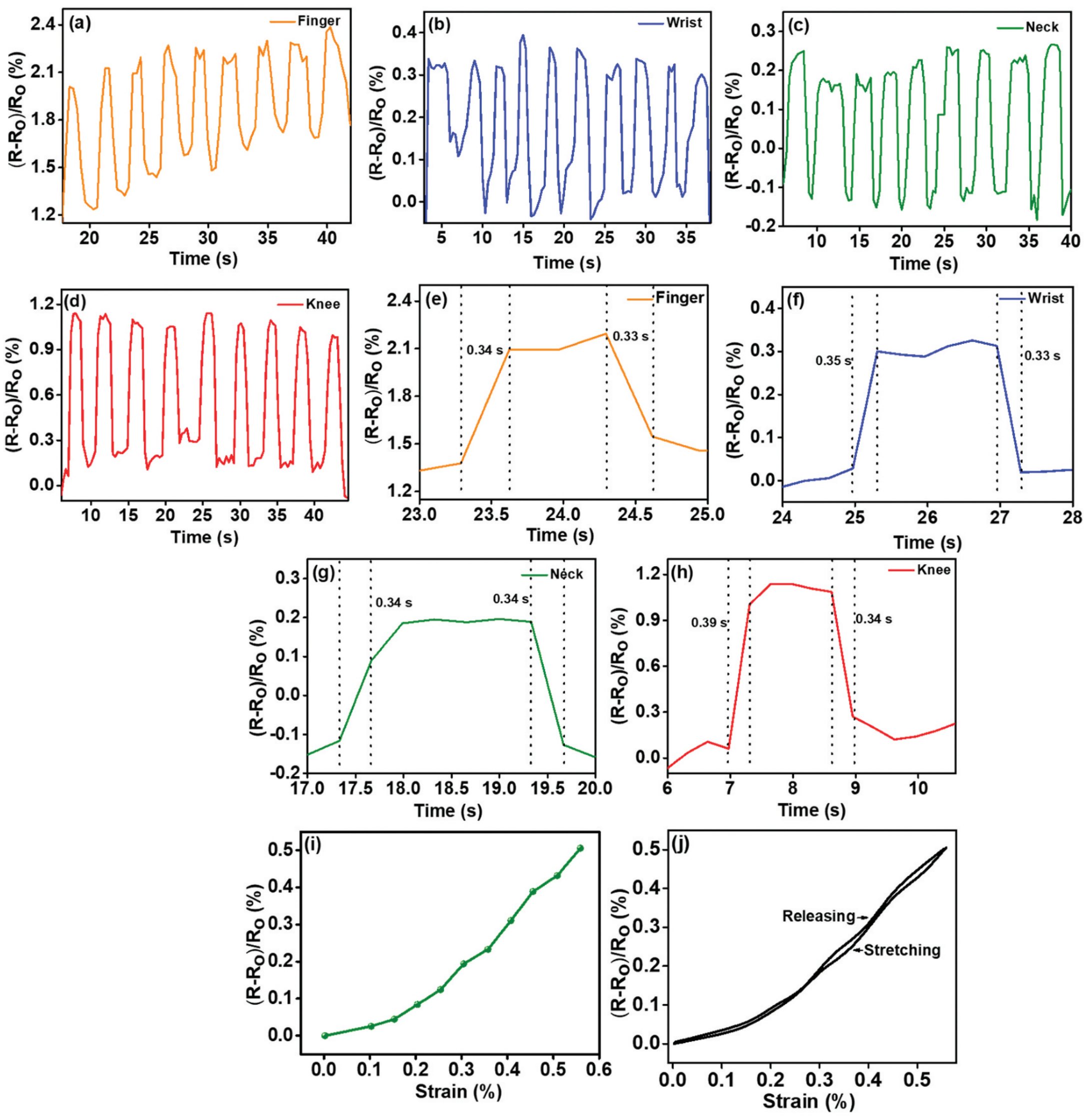

Figure 5. (a–d) Performance of the GO/(10%) CuO-coated Hanji-based wearable strain sensor in monitoring human motion; (e–h) Response and recovery time of Hanji-based wearable strain sensor in monitoring human motion and (i–j) Gauge factor and relative change in resistance of GO/CuO-Hanji when applied 0 to 0.5 % strain.

Hanji exhibited excellent retention performance, maintaining 100% of its initial heating capability even after 100 repeated Joule heating cycles (Figure S3), indicating strong operational durability. A systematic investigation on the GO-to-rGO transition and its impact on device performance will be addressed in future work.

In GO/(10%)CuO-coated Hanji, the strain sensor and Joule heater functionalities coexist without interference due to the stable percolation network of GO/CuO. The stain sensing and joule heating mechanism of GO/CuO-coated Hanji is given Figure 6. In strain sensing mode, resistance variation is primarily influenced by mechanical deformation, where stretching or releasing alters the conduction pathways. However, in Joule heating mode, a stable voltage is applied across the GO/CuO network, ensuring consistent power dissipation ($p = V^2/R$) for uniform heat generation (Wu et al. 2024). The heating mechanism is governed by electron

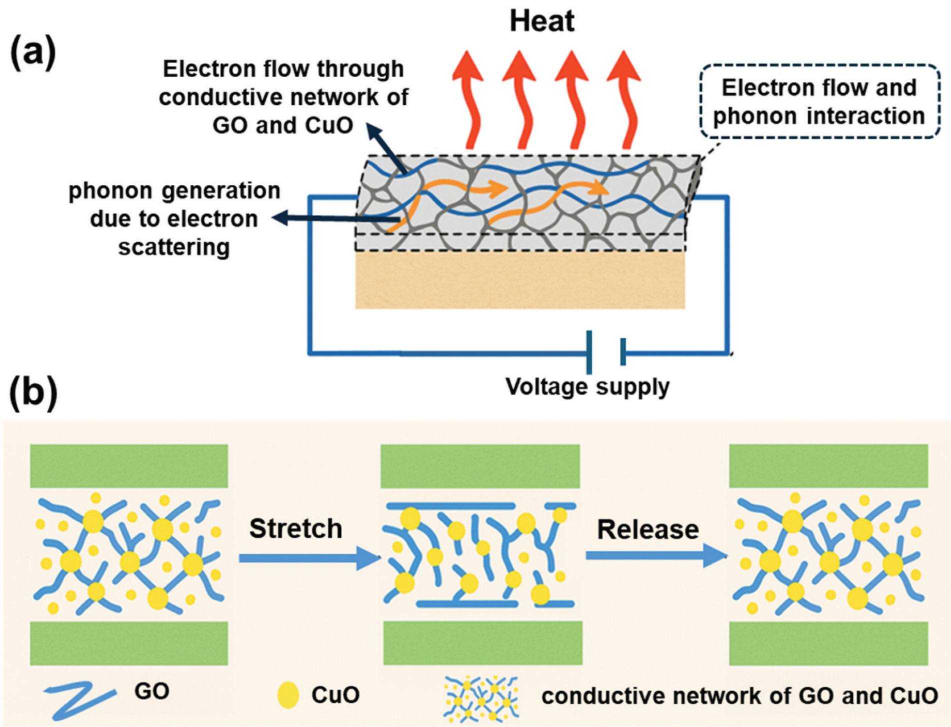

Figure 6. (a) Joule heating and (b) strain sensing mechanism of GO/(10%)CuO-coated hanji.

flow through the conductive network, where electron scattering generates phonons, leading to thermal energy release. The Joule heating behavior of the GO/(10%)CuO-coated Hanji-based wearable heater is dominated by the bulk resistance of the material, which does not undergo drastic changes under moderate strain. Furthermore, the high thermal conductivity of GO enables efficient heat distribution, preventing localized overheating due to minor resistance variations. A photographic image of the GO/CuO-coated Hanji paper is provided in the Supporting Information (Fig. S4), offering a visual representation of the coating uniformity. Thus, the GO/(10%)CuO-coated Hanji-based strain sensor and Joule heater operate independently, ensuring reliable strain detection without compromising thermal stability.

Conclusion

The GO/CuO-coated Hanji papers developed in this study successfully integrated excellent electrical conductivity, thermal stability, and multifunctionality, making them potential alternatives for wearable, flexible thermal heaters. The synergistic interaction between GO and 10% CuO significantly enhanced the Joule heating performance, achieving rapid and uniform heating. At an applied voltage of 30 V, the heater reached a surface temperature of 80 °C within 180 s. Furthermore, its outstanding thermal stability was demonstrated by its consistent performance over 30 min without a decrease, highlighting the potential of GO/(10%)CuO-coated Hanji as a reliable and efficient thermal heater for diverse applications. The Hanji-based heater maintained its heating performance across various bending angles, highlighting its mechanical flexibility, which is critical for wearable devices. In addition to Joule heating, the GO/CuO-coated Hanji exhibited excellent deicing performance and functioned as a wearable strain sensor for detecting human physiological movements. These findings confirm the cost-effectiveness and eco-friendliness of GO/CuO-coated Hanji, making it a promising solution for next-generation wearable electronics, smart textiles, thermal management systems, and deicing technologies.

Highlights

- Hanji-based electrode is fabricated by screen printing for eco-friendly, lightweight, and flexible solutions for wearable applications.
- The incorporation of GO/CuO coatings significantly enhances conductivity and joule heating performance.
- The thermal heaters achieve a surface temperature of approximately 80 °C within 180 seconds.
- The multifunctional capabilities with deicing and wearable sensing capabilities are demonstrated.

Acknowledgments

This work was supported by the National Research Foundation of Korea (NRF) grant funded by the Korea government (MSIT) (RS-2024-00413272). This work was supported by the National Research Foundation of Korea (NRF) grant funded by the Government of Korea (NRF-RS-2024-00336593). This work was supported by BK21 FOUR Program by Jeonbuk National University Research Grant. This work was also supported by the University of Glasgow Startup Fund.

Disclosure statement

No potential conflict of interest was reported by the author(s).

Funding

This work was supported by the Chung-Ang University [2024].

References

Aier, I., and D. Dhar Purkayastha. 2025. “Dual Role of cuo Nanoparticles on Melamine Sponge: Oil-Water Separation and Photocatalytic Dye Removal.” *Chemical Physics Letters* 867:142000. https://doi.org/10.1016/j.cplett.2025.142000.

Akram, S., M. Ashraf, H. Aziz, A. Farooq, A. Imran, A. Javid, S. Ali, et al. 2024. “Fabrication of Copper Coated Aminated Graphene Oxide Based Textiles for Electromagnetic Interference Shielding Applications.” *Diamond and Related Materials* 150:111729. https://doi.org/10.1016/j.diamond.2024.111729.

Chen, W., S. Yang, H. Wang, K. Yang, X. Wu, F. Gao, et al. 2022. “Flexible, Stretchable, Waterproof (IPX7) Electro-Thermal Films Based on Graphite Nanoplatelets & Polyurethane Nanocomposites for Wearable Heaters.” *Chemical Engineering Journal* 431:133990. https://doi.org/10.1016/j.cej.2021.133990.

Cheng, R., B. Wang, J. Zeng, J. Li, J. Xu, W. Gao, K. Chen, et al. 2022. “High-Performance and Rapid-Response Electrical Heaters Derived from Cellulose Nanofiber/Silver Nanowire Nanopapers for Portable Thermal Management.” *ACS Applied Materials & Interfaces* 14 (26): 30144–30159. https://doi.org/10.1021/acsami.2c04931.

Chien, A.-T., S. Cho, Y. Joshi, and S. Kumar. 2014. “Electrical Conductivity and Joule Heating of Polyacrylonitrile/Carbon Nanotube Composite Fibers.” *Polymer* 55 (26): 6896–6905. https://doi.org/10.1016/j.polymer.2014.10.064.

Choi C, Qaiser N and Hwang B. (2024). MECHANICALLY PRESSED POLYMER-MATRIX COMPOSITES WITH 3D STRUCTURED FILLER NETWORKS FOR ELECTROMAGNETIC INTERFERENCE SHIELDING APPLICATION. FU Mech Eng, 601 10.22190/FUME240601038C

Choi, S., J. Park, W. Hyun, J. Kim, J. Kim, Y. B. Lee, C. Song, et al. 2015. “Stretchable Heater Using Ligand-Exchanged Silver Nanowire Nanocomposite for Wearable Articular Thermotherapy.” *ACS Nano* 9 (6): 6626–6633. https://doi.org/10.1021/acsnano.5b02790.

Dou, W., J. Wu, T. Gu, P. Wang, and D. Zhang. 2018. “Preparation of Super-Hydrophobic Micro-Needle cuo Surface as a Barrier Against Marine Atmospheric Corrosion.” *Corros Sci* 131:156–163. https://doi.org/10.1016/j.corsci.2017.11.012.

Fang, S., R. Wang, H. Ni, H. Liu, and L. Liu. 2022. “A Review of Flexible Electric Heating Element and Electric Heating Garments.” *Journal of Industrial Textiles* 51 (1_suppl): 101S–136S. https://doi.org/10.1177/1528083720968278.

Faruk, M. O., A. Ahmed, M. A. Jalil, M. T. Islam, A. M. Shamim, B. Adak, M. M. Hossain, et al. 2021. “Functional Textiles and Composite Based Wearable Thermal Devices for Joule Heating: Progress and Perspectives.” *Applied Materials Today* 23:101025. https://doi.org/10.1016/j.apmt.2021.101025.

Ganesan, K., V. K. Jothi, A. Natarajan, A. Rajaram, S. Ravichandran, and S. Ramalingam. 2020. "Green Synthesis of Copper Oxide Nanoparticles Decorated with Graphene Oxide for Anticancer Activity and Catalytic Applications." *Arabian Journal of Chemistry* 13 (8): 6802–6814. https://doi.org/10.1016/j.arabjc.2020.06.033.

Griffin, A., M. Robertson, Z. Gunter, A. Coronado, Y. Xiang, and Z. Qiang. 2024. "Design and Application of Joule Heating Processes for Decarbonized Chemical and Advanced Material Synthesis." *Industrial & Engineering Chemistry Research* 63 (45): 19398–19417. https://doi.org/10.1021/acs.iecr.4c02460.

Ha H, Mueller S, Guriyanova S and Hwang B. (2025). SURFACE ENERGY CHARACTERIZATION OF A SINGLE MICROSPHERE PARTICLE USING PEAKFORCE QUANTITATIVE NANOMECHANICAL MAPPING MODE OF ATOMIC FORCE MICROSCOPE. FU Mech Eng, 171 10.22190/FUME250114012H

Ha H, Müller S, Baumann R and Hwang B. (2024). PEAKFORCE QUANTITATIVE NANOMECHANICAL MAPPING FOR SURFACE ENERGY CHARACTERIZATION ON THE NANOSCALE: A MINI-REVIEW. FU Mech Eng, 22 (1), 001 10.22190/FUME221126001H

Ha H, Qaiser N, Yun T Gwang, Cheong J Young, Lim S and Hwang B. (2023). SENSING MECHANISM AND APPLICATION OF MECHANICAL STRAIN SENSOR: A MINI-REVIEW. FU Mech Eng, 21(4), 751 10.22190/FUME230925043H

Han, T.-H., H. Kim, S.-J. Kwon, and T.-W. Lee. 2017. "Graphene-Based Flexible Electronic Devices." *Materials Science and Engineering: R: Reports* 118:1–43. https://doi.org/10.1016/j.mser.2017.05.001.

Han, Y., H. Ha, T. Suryaprabha, P. Baumli, and B. Hwang. 2024. "Mulberry-Paper-Based Electrodes with Hybrid Nanocomposite Coatings and Their Application to Eco-Friendly Energy-Storage Devices." *Cellulose* 31 (3): 1675–1685. https://doi.org/10.1007/s10570-023-05701-y.

Hu, Z., J. Zhou, and Q. Fu. 2021. "Design and Construction of Deformable Heaters: Materials, Structure, and Applications." *Advanced Electronic Materials* 7 (11). https://doi.org/10.1002/aelm.202100459.

Huang, Z., S. Li, H. Guo, C. Huang, Y. Bian, Y. Gong, J. Huang, et al. 2023. "Multi-Scale go/CNT/AlN Nanocomposites for High-Performance Flexible Electrothermal Film Heaters." *Journal of Materials Chemistry C* 11 (29): 9925–9936. https://doi.org/10.1039/D3TC01265D.

Jeong, J., H.-J. Seok, H. Shin, S. Choi, J.-W. Kim, and H.-K. Kim. 2024. "Highly Durable and Conductive Korea Traditional Paper (hanji) Embedded with Ti3C2Tx MXene for Hanji-Based Paper Electronics." *Nano Energy* 131:110325. https://doi.org/10.1016/j.nanoen.2024.110325.

Jiang, H., H. Wang, G. Liu, Z. Su, J. Wu, J. Liu, X. Zhang, et al. 2017. "Light-Weight, Flexible, Low-Voltage Electro-Thermal Film Using Graphite Nanoplatelets for Wearable/Smart Electronics and Deicing Devices." *Journal of Alloys and Compounds* 699:1049–1056. https://doi.org/10.1016/j.jallcom.2016.12.435.

Jiang, X., R. Zhang, T. Yang, S. Lin, Q. Chen, Z. Zhen, D. Xie, et al. 2016. "Foldable and Electrically Stable Graphene Film Resistors Prepared by Vacuum Filtration for Flexible Electronics." *Surface and Coatings Technology* 299:22–28. https://doi.org/10.1016/j.surfcoat.2016.04.066.

Jitjaicham, M., and B. Kusuktham. 2016. "Preparation of Paper Mulberry Fibers and Possibility of cotton/Paper Mulberry Yarns Production." *Indian Journal of Materials Science* 2016:1–6. https://doi.org/10.1155/2016/1498967.

Khadka, A., B.-Y. Kim, C. Park, W. Lim, A. Aldalbahi, G. Periyasami, B. Joshi, et al. 2023. "Eco-Friendly Cellulose Wearable Heaters Using Korean Traditional Han Paper Coated with Graphene Nanosheets via Binder-Free Supersonic Spraying." *Physics of Fluids* 35 (5). https://doi.org/10.1063/5.0148669.

Khadka, A., B.-Y. Kim, S. Pradhan, C. Park, W. Lim, A. Aldalbahi, G. Periyasami, et al. 2023. "Silver–Nickel Core–Shell Nanostructure on Cellulose Fibers as Biodegradable Wearable Paper Heater." *Cellulose* 30 (10): 6559–6569. https://doi.org/10.1007/s10570-023-05250-4.

Khuje, S., L. Zhu, J. Yu, and S. Ren. 2024. "copper-Coated e-Glass fiber-Based Strain Sensors for High Temperatures." *ACS Applied Electronic Materials* 6 (11): 8226–8231. https://doi.org/10.1021/acsaelm.4c01510.

Kim, C.-L., J.-J. Lee, Y.-J. Oh, D.-E. Kim. 2017. "Smart Wearable Heaters with High Durability, Flexibility, Water-Repellent and Shape Memory Characteristics." *Composites Science and Technology* 152:173–180. https://doi.org/10.1016/j.compscitech.2017.09.023.

Kim H, Qaiser N and Hwang B. (2023). ELECTRO-MECHANICAL RESPONSE OF STRETCHABLE PDMS COMPOSITES WITH A HYBRID FILLER SYSTEM. FU Mech Eng, 21(1), 051 10.22190/FUME221205002K

Kim, H., A. P. Tiwari, and H. Y. Kim. 2021. "Fabrication of Electrically Highly Conductive, Mechanically Strong, and Near-Infrared Responsive Phytic Acid Crosslinked Polypyrrole Coated Korean Paper." *Materials Today Communications* 26:102081. https://doi.org/10.1016/j.mtcomm.2021.102081.

Kim, J., Y. Choi, H. Jang, S. Jiong, X. Chen, B. Seo, W. Choi, et al. 2024. "Thermo-Chemo-Mechanically Robust, Multifunctional MXene/PVA/PAA-Hanji Textile with Energy Harvesting, EMI Shielding, flame-Retardant, and Joule Heating Capabilities." *Advanced Materials* 36 (47): 2411248. https://doi.org/10.1002/adma.202411248.

Kim, Y. J., S. Y. Choi, H. Shin, and H. K. Kim. 2023. "Conductive Korean Traditional Paper (hanji) Coupled with Ag Nanowire for Functional Electronic Paper Windows in Hanok." *Advanced Materials Technologies* 8 (12): 2202015. https://doi.org/10.1002/admt.202202015.

Kim, Y. J., S. Yoon, Y.-H. Cho, G. Kim, and H.-K. Kim. 2020. "Paintable and Writable Electrodes Using Black Conductive Ink on Traditional Korean Paper (hanji)." *RSC Advances* 10 (41): 24631–24641. https://doi.org/10.1039/D0RA04412A.

Kiran Kumar, S. R., G. P. Mamatha, H. B. Muralidhara, M. S. Anantha, S. Yallappa, B. S. Hungund, K. Yogesh Kumar, et al. 2017. "Highly Efficient Multipurpose Graphene Oxide Embedded with Copper Oxide Nanohybrid for Electrochemical Sensors and Biomedical Applications." *Journal of Science: Advanced Materials and Devices* 2 (4): 493–500. https://doi.org/10.1016/j.jsamd.2017.08.003.

Krishnamoorthy, K., M. Veerapandian, K. Yun, and S.-J. Kim. 2013. "The Chemical and Structural Analysis of Graphene Oxide with Different Degrees of Oxidation." *Carbon* 53:38–49. https://doi.org/10.1016/j.carbon.2012.10.013.

Lee, D., G. Bang, M. Byun, and D. Choi. 2020. "Highly Flexible, Transparent and Conductive Ultrathin Silver Film Heaters for Wearable Electronics Applications." *Thin Solid Films* 697:697. https://doi.org/10.1016/j.tsf.2020.137835.

Lee, Y. J., S. Y. Won, S. B. Park, and H.-J. Kim. 2024. "Chemometric Approaches for Discriminating Manufacturers of Korean Handmade Paper Using Infrared Spectroscopy." *Heritage Science* 12 (1): 12. https://doi.org/10.1186/s40494-024-01460-6.

Lim, W., A. Khadka, B.-Y. Kim, C. Park, A. Aldalbahi, G. Periyasami, B. Joshi, et al. 2023. "Wearable Heater Composites Comprising Traditional Hanji Cellulose Fibers Coated with Graphene, Silver Nanowires, and PEDOT: PSS via Scalable Supersonic Spraying." *Journal of Materials Science & Technology* 164:27–36. https://doi.org/10.1016/j.jmst.2023.04.028.

Lin, S.-Y., T.-Y. Zhang, Q. Lu, D.-Y. Wang, Y. Yang, X.-M. Wu, T.-L. Ren, et al. 2017. "High-Performance Graphene-Based Flexible Heater for Wearable Applications." *RSC Advances* 7 (43): 27001–27006. https://doi.org/10.1039/C7RA03181E.

Liu, Q., B. Tian, J. Liang, and W. Wu. 2021. "Recent Advances in Printed Flexible Heaters for Portable and Wearable Thermal Management." *Materials Horizons* 8 (6): 1634–1656. https://doi.org/10.1039/D0MH01950J.

Liu, Q., B. Tian, C. Luo, J. Liang, and W. Wu. 2020. "Printed Flexible heaters-Based Thermotherapy Platform for Multiduty Thermal Management." *Advanced Materials Technologies* 5 (8). https://doi.org/10.1002/admt.202000278.

Mathesh, M., J. Liu, N. D. Nam, S. K. H. Lam, R. Zheng, C. J. Barrow, W. Yang, et al. 2013. "Facile Synthesis of Graphene Oxide Hybrids Bridged by Copper Ions for Increased Conductivity." *Journal of Materials Chemistry C* 1 (18): 3084–3090. https://doi.org/10.1039/c3tc30180j.

Mathesh, M., J. Liu, N. D. Nam, S. K. H. Lam, R. Zheng, C. J. Barrow, W. Yang, et al. 2013. "Facile Synthesis of Graphene Oxide Hybrids Bridged by Copper Ions for Increased Conductivity." *Journal of Materials Chemistry C* 1 (18): 1. https://doi.org/10.1039/c3tc30180j.

Menazea, A., and M. Ahmed. 2020. "Synthesis and Antibacterial Activity of Graphene Oxide Decorated by Silver and Copper Oxide Nanoparticles." *Journal of Molecular Structure* 1218:128536. https://doi.org/10.1016/j.molstruc.2020.128536.

Rajak, C., S. Pramanik, S. Das, S. Santra, R. Mandal, S. Dey, R. Nath, et al. 2024. "Evolution of Phase, Surface Morphology and Wettability of Sputtered Copper Thin Films on Annealing in Air: Formation of cuo/Cu2O/Cu Nanocomposites." *Surfaces and Interfaces* 55:55. https://doi.org/10.1016/j.surfin.2024.105459.

Rostami, S., A. A. Nadooshan, A. Raisi, and M. Bayareh. 2021. "Modeling the Thermal Conductivity Ratio of an Antifreeze-Based Hybrid Nanofluid Containing Graphene Oxide and Copper Oxide for Using in Thermal Systems." *Journal of Materials Research and Technology* 11:2294–2304. https://doi.org/10.1016/j.jmrt.2021.02.044.

Seo, Y., and B. Hwang. 2019. "Mulberry-Paper-Based Composites for Flexible Electronics and Energy Storage Devices." *Cellulose* 26 (16): 8867–8875. https://doi.org/10.1007/s10570-019-02686-5.

Shi, Y., C. Wang, Y. Yin, Y. Li, Y. Xing, and J. Song. 2019. "Functional Soft Composites as Thermal Protecting Substrates for Wearable Electronics." *Advanced Functional Materials* 29 (45). https://doi.org/10.1002/adfm.201905470.

Shin, S., S. Park, A. Toor, and H. So. 2023. "Heating Performance, fabrication, and Characterization of Functional Electrothermal Heaters Built from Cellulose." *Cellulose* 30 (10): 6119–6147. https://doi.org/10.1007/s10570-023-05264-y.

Singh, P., P. Nath, R. K. Arun, S. Mandal, and N. Chanda. 2016. "Novel Synthesis of a Mixed cu/cuo–Reduced Graphene Oxide Nanocomposite with Enhanced Peroxidase-Like Catalytic Activity for Easy Detection of Glutathione in Solution and Using a Paper Strip." *RSC Advances* 6 (95): 92729–92738. https://doi.org/10.1039/C6RA20882G.

Souri, H., H. Banerjee, A. Jusufi, N. Radacsi, A. A. Stokes, I. Park, M. Sitti, et al. 2020. "Wearable and Stretchable Strain Sensors: Materials, Sensing Mechanisms, and Applications." *Advanced Intelligent Systems* 2 (8). https://doi.org/10.1002/aisy.202000039.

Suryaprabha, T., and S. Park. 2023. "Fabrication of Multifunctional Cotton Textile with Battery Waste-Derived Graphene Oxide for Enhanced Joule Heating and Electromagnetic Interference Shielding." *Journal of Industrial Textiles* 53:15280837231178945. https://doi.org/10.1177/15280837231178945.

Suryaprabha, T., and M. G. Sethuraman. 2017. "Fabrication of Copper-Based Superhydrophobic Self-Cleaning Antibacterial Coating Over Cotton Fabric." *Cellulose* 24 (1): 395–407. https://doi.org/10.1007/s10570-016-1110-z.

Tembei, S. A. N., A. Hessein, A. M. R. Fath El-Bab, and A. A. El-Moneim. 2020. "A Low Voltage, Flexible, Graphene-Based Electrothermal Heater for Wearable Electronics and Localized Heating Applications." Materials Today: Proceedings;33, 1840–1844.

Tiwari, N., A. Ankit, M. R. Rajput, M. R. Kulkarni, R. A. John, and N. Mathews. 2017. "Healable and Flexible Transparent Heaters." *Nanoscale* 9 (39): 14990–14997. https://doi.org/10.1039/C7NR05748B.

Ullah, H. M. K., J. Lejeune, A. Cayla, M. Monceaux, C. Campagne, and É. Devaux. 2022. "A Review of Noteworthy/ Major Innovations in Wearable Clothing for Thermal and Moisture Management from Material to Fabric Structure." *Textile Research Journal* 92 (17–18): 3351–3386. https://doi.org/10.1177/00405175211027799.

Verma, S., and R. K. Dutta. 2015. "A Facile Method of Synthesizing Ammonia Modified Graphene Oxide for Efficient Removal of Uranyl Ions from Aqueous Medium." *RSC Advances* 5 (94): 77192–77203. https://doi.org/10.1039/C5RA10555B.

Vertuccio, L., F. De Santis, R. Pantani, K. Lafdi, and L. Guadagno. 2019. "Effective de-Icing Skin Using Graphene-Based Flexible Heater." *Composites Part B: Engineering* 162:600–610. https://doi.org/10.1016/j.compositesb.2019.01.045.

Wang, B., H. Cheng, J. Zhu, Y. Yuan, and C. Wang. 2020. "A Flexible and Stretchable Polypyrrole/Knitted Cotton for Electrothermal Heater." *Organic Electronics* 85:105819. https://doi.org/10.1016/j.orgel.2020.105819.

Wu, T., S. Ren, W. Akram, T. Li, X. Zhu, X. Li, L. Niu, et al. 2024. "high-Performance Wearable Joule Heater Derived from sea–Island Microfiber Nonwoven Fabric." *ACS Applied Materials & Interfaces* 16 (38): 51565–51574. https://doi.org/10.1021/acsami.4c13386.

Xiang, D., L. Liu, F. Xu, Y. Li, E. Harkin-Jones, Y. Wu, C. Zhao, et al. 2023. "Highly Sensitive Flexible Strain Sensor Based on a Double-Percolation Structured Elastic Fiber of Carbon Nanotube (cnt)/Styrene Butadiene Styrene (SBS)@ Thermoplastic Polyurethane (TPU) for Human Motion and Tactile Recognition." *Applied Composite Materials* 30 (1): 307–322. https://doi.org/10.1007/s10443-022-10084-7.

Xie, S., T. Li, Z. Xu, Y. Wang, X. Liu, and W. Guo. 2018. "A High-Response Transparent Heater Based on a cus Nanosheet Film with Superior Mechanical Flexibility and Chemical Stability." *Nanoscale* 10 (14): 6531–6538. https://doi.org/10.1039/C7NR09667D.

Xu, C., X. Wang, L. Yang, and Y. Wu. 2009. "Fabrication of a Graphene–Cuprous Oxide Composite." *Journal of Solid State Chemistry* 182 (9): 2486–2490. https://doi.org/10.1016/j.jssc.2009.07.001.

Yasin, G., M. Arif, M. Shakeel, Y. Dun, Y. Zuo, W. Q. Khan, Y. Tang, et al. 2018. "Exploring the nickel–Graphene Nanocomposite Coatings for Superior Corrosion Resistance: Manipulating the Effect of Deposition Current Density on Its Morphology, Mechanical Properties, and erosion-Corrosion Performance." *Advanced Engineering Materials* 20 (7): 20. https://doi.org/10.1002/adem.201701166.

Yu, H., X. Yang, Y. Lian, M. Wang, Y. Liu, Z. Li, Y. Jiang, et al. 2021. "An Integrated Flexible Multifunctional Wearable Electronic Device for Personal Health Monitoring and Thermal Management." *Sensors and Actuators A: Physical* 318:112514. https://doi.org/10.1016/j.sna.2020.112514.

Yun, T. G., D. Kim, S. M. Kim, I. D. Kim, S. Hyun, and S. M. Han. 2018. "Mulberry paper-Based Supercapacitor Exhibiting High Mechanical and Chemical Toughness for large-Scale Energy Storage Applications." *Advanced Energy Materials* 8 (21). https://doi.org/10.1002/aenm.201800064.

Zeng, Q., L. Zhang, J. Zhang, and A. Zhang. 2023. "Thermo-Conductive, Air-Permeable, and Hydrophobic Sulfonated Poly (Styrene-Ethylene/butylene-Styrene)/boron Nitride Nanosheet Nanofiber Membranes for Wearables via One-Step Electrospinning." *ACS Applied Polymer Materials* 5 (7): 4868–4878. https://doi.org/10.1021/acsapm.3c00352.

Zhou, C., F. Qing, X. Sun, R. Wu, H. Wang, Q. Wen, X. Li, et al. 2024. "Preparation of Graphene-Coated Cu Particles with Oxidation Resistance by Flash Joule Heating." *Carbon* 224:224. https://doi.org/10.1016/j.carbon.2024.119060.